Eur Biophys J (1998) 27: 582–589

ARTICLE

C. Otto · N. M. Sijtsema · J. Greve

Confocal Raman microspectroscopy of the activation of single neutrophilic granulocytes

Received: 1 September 1998 / Revised version: 20 February 1998 / Accepted: 22 February 1998

Abstract Confocal Raman micro-spectroscopy has been applied to investigate the activation process of single, living neutrophilic granulocytes. Both resting cells as well as activated cells were measured. The activation of cells was performed with phorbol-12-myristate-13-acetate activator and Escherichia Coli bacteria. Raman microspectroscopy combines a high spatial resolution inside a single, living cell with detailed material information. Using this approach it can be concluded that activation of the cells with phorbol-12-myristate-13-acetate causes a change in the redox state of cytochrome b_{558}. This protein is a part of the NADPH-oxidase complex that neutrophilic granulocytes employ to generate O_2^-, superoxide anion. Additionally a change in the redox state of myeloperoxidase can be observed. Myeloperoxidase is known to react with O_2^-. Activation of the cells with bacteria gives rise to corresponding changes in the Raman spectra. From this single cell study it can be concluded that the enzymes cytochrome b_{558} and myeloperoxidase are present inside the cytoplasm of the living cell, while participating in the redox processes. Activation causes an intra-cellular release of oxygen metabolites. Activation with bacteria of neutrophilic granulocytes from a patient with chronic granulomatous disease, that contain no cytochrome b_{558}, led to typical changes in the redox state of myeloperoxidase. This indicates that in the bacterium/neutrophilic granulocyte system oxygen metabolites are generated that are capable of reacting with MPO.

Key words Raman · Confocal · Microspectroscopy · Neutrophilic · Granulocyte

C. Otto (✉) · N. M. Sijtsema · J. Greve
University of Twente, Department of Applied Physics,
Biophysical Technology Group,
Institute for BioMedical Technology, P. O. Box 217,
7500 AE Enschede, The Netherlands
e-mail: c.otto@tn.utwente.nl

Introduction

Phagocytosis is the process that enables various animal cells, predominantly the granulocytes, monocytes and macrophages, to approach, recognize, engulf and destroy bacteria and viruses. In this way these cells play a vital role in the immune response of the body against harmful invaders. The granulocytes, i. e. neutrophilic, eosinophilic and basophilic cells, prepare potent chemicals for the destruction of the body-strange material in the phagosome. These chemicals are well to auto-degrade the granulocyte. Proper timing of the production and localization of these chemicals is therefore vital to the cell. The enzymes required to produce agents with bactericidal effects are present in granules, inside the cytoplasm. We will concentrate in this paper on experiments performed on neutrophilic granulocytes. The neutrophils are probably the most active granulocytes in killing bacteria. Neutrophilic granulocytes contain three morphologically distinct types of granules, the azurophilic, the specific and the nucleated granules (Brederoo et al. 1983). The azurophilic granules contain myeloperoxidase (MPO), while the specific neutrophils react negatively to peroxidase staining. The specific granules contain (a part of) the nicotinamide adenine dinucleotide phosphate (NADPH)-oxidase complex. This complex utilizes NADPH as an electron donor and transfers the electrons to molecular oxygen. It is presently thought (Bjerrum and Borregaard 1989; Jesaitis et al. 1990) that a granule-membrane associated protein complex, containing both a protein that contains flavine adenine dinucleotide (FAD) and a protein that contains a cytochrome, forms an important part of the NADPH-oxidase system. The cytochrome containing protein from the NADPH-oxidase complex is called cytochrome b_{558} (Cb_{558}). The superoxide anion (O_2^-) produced is in itself a potent killer. In order to generate sufficient O_2^- the neutrophilic granulocyte increases its oxygen consumption, the so called respiratory burst (Babior 1978). The O_2^- is transformed to hydrogen peroxide (H_2O_2) by superoxide dismutase. Hydrogen peroxide in turn is a substrate for MPO under the formation of compound I

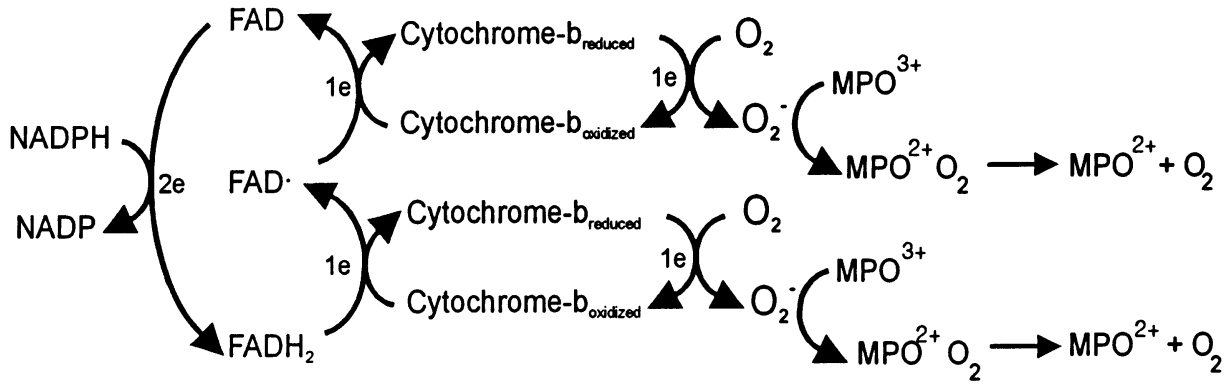

Fig. 1 A schematic overview of the reactions of the NADPH-oxidase complex and myeloperoxidase. On the left-hand side, on the cytosolic side of the membrane, NADPH is supplying electrons that are accepted by the FAD group and transferred to the cytochrome b_{558} group in the NADPH-oxidase complex. On the phagosomal side the electrons are accepted by molecular oxygen to form O_2^--anion. Native myeloperoxidase (MPO^{3+}) may next react with superoxide to form $MPO^{2+}O_2$ (compound III), which converts to reduced myeloperoxidase (MPO^{2+}) with the release of molecular oxygen. The NADPH-oxidase complex is a transmembrane protein and myeloperoxidase is released from the azurophilic granules in the phagosome

(Marquez et al. 1994). Compound I has a sufficiently high redox potential that it can oxidize chloride anions to hypohalous acid, a strong acid that is killing and degrading the bacteria in the phagosome, and the reverse reaction of compound I to MPO. However, O_2^- also reacts directly with MPO to form compound III. Compound III dissociates into molecular oxygen and reduced MPO. In Fig. 1 a schematic view is presented of the molecular reactions in this process.

Raman spectroscopy is a laser based type of spectroscopy that presents information on the vibrational states of molecules (Long 1977). The spectral information is generated in a Raman scattering process of the light from the molecules in the object. A small fraction of the scattered light is shifted in frequency with respect to the original laser frequency, which has a narrow bandwidth. The frequency shift is a result of the internal, i. e. vibrational and (when the object is in a gaseous phase) rotational dynamics of the molecules. Different molecules have different vibrational states and they can therefore be distinguished with this technique. An important aspect of the method is that it can easily be combined with optical light microscopes. In this configuration Raman microspectroscopy benefits from all the possibilities of optical microscopes, i. e. the ease of alignment, the ability to visualize the sample before and after a measurement and the high resolution through the confocal measurement principle. Raman microspectroscopy of single cells demands a high quality of the optical components of the Raman microspectrometer. These high demands are a direct consequence of the low signal strengths. When these demands are met, Raman microspectroscopy combines a high resolution with a high information content and does not require may staining of the sample.

In principle the Raman spectra of cells are very complicated because of the overlapping spectra of an enormous number of molecular compounds present in the cells. In this particular study we have employed resonant Raman microspectroscopy (Long 1977) to obtain only the signals of Cb_{558} and MPO. The selectivity arises from the fact that the frequency of the light of the exciting laser line is in resonance with an electronic transition of the enzymatic complex. The resonance Raman scattering gives rise to a much higher signal from this complex than from the non-resonantly excited majority of molecules. Raman light scattering can measure the changes in the redox state of the porphyrin prosthetic groups in the enzymes Cb_{558} and MPO. This paper will present the results of the changes of cytochrome b_{558} and myeloperoxidase inside single, living neutrophilic granulocytes.

Various diseases are related to the lack of activity of Cb_{558} or MPO. The most serious consequences arise from a in ability to form superoxide radicals. This may result from genetic defects in any of the proteins participating in the NADPH-oxidase complex. The defects in the NADPH-oxidase complex lead to the occurrence of chronic granulomatous disease (CGD) (Cross and Curnutte 1995; Cross et al. 1995). Patients that have a MPO deficiency suffer, usually, less severe consequences (Nauseef 1990). Cells from a patient with CGD and from a patient with a MPO deficiency have been included in this study.

Materials and methods

The neutrophilic granulocytes used in single cell Raman microspectroscopy were isolated from fresh heparinized blood as described previously (Yazdanbakhsh et al. 1987). Quartz plates were incubated overnight with 0.01% poly-L-lysine (PLL, Sigma, P-1274) in PBS at 4 °C. A few drops of ($2*10^6$) neutrophils/ml suspended in RPMI 1640+ 25 mM HEPES without phenolred (Seromed) with 3% Fetal Calf Serum (FCS, Gibco 011-06180) were put on a quartz plate coated with PLL. After an incubation of 10 min at 37 °C the cells stuck to the quartz and the quartz plate was placed in a petri-dish (3.5 mm) and 2 ml RPMI + FCS was added. During the measurements the sample was kept at 37 °C. The neutrophilic granulocytes used in the absorp-

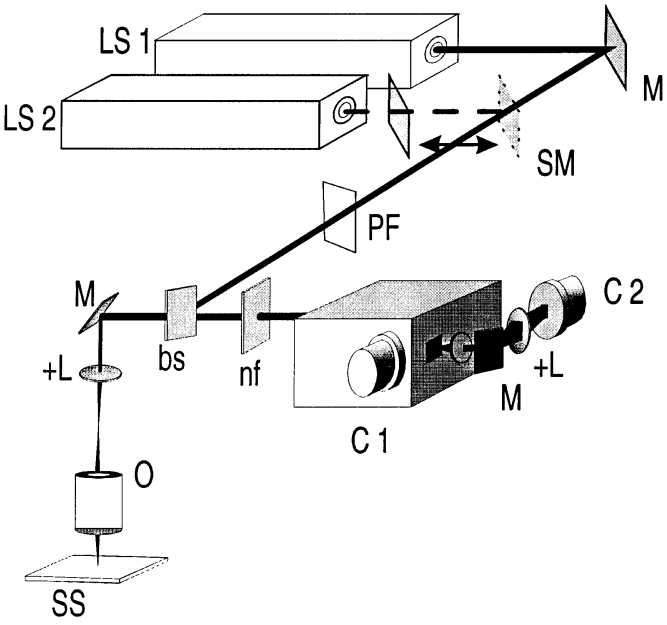

Fig. 2 A schematic view of the Raman microspectrometer. The microscope section is symbolized by the objective (O) only. This section also enables us to visualize the object, on the sample stage (SS), with "ordinary" (bright field, dark field, polarization contrast) microscope techniques. The setup further consists of an Ar^+-ion (LS1) and a Kr^+-ion (LS2) laser light source, providing a range of excitation wavelengths from the "blue" through the "green" to the "red". The lasers can use the same light path with the help of mirrors (M) and sliding mirror (SM). A plasma filter (PF) effectively attenuates plasma emission from the lasers. Important for the working of the Raman microspectrometer is the quality of the beam-splitter (BS) and the filter for the laser wavelength suppression (NF). The scattered light is imaged on the entrance pinhole (50 μm) by a lens (not visible) with a focal length of 35 mm. The polychromator disperses the light and images the spectrum on a CCD camera (C1). Raman imaging is also possible with this setup (Sijtsema et al. 1998). The alternative exit port of the polychromator is used in that case. The microscope objective is completely filled by lens (L) with a focal length of 100 mm

tion measurements were obtained from peripheral blood and isolated from buffycoats of the local Central Blood bank (Enschede) (Yazdanbakhsh et al. 1987). 2.5 ml of $5*10^7$ cells/ml in medium 1 were put in a quartz cuvette (Hellma Standard Cuvet 110 QS).

Specific and azurophilic granule fractions were obtained after sonication of neutrophils followed by discontinuous sucrose gradient centrifugation (15/40/52/60% weight/volume sucrose) (Bolscher et al. 1990).

The neutrophilic granulocytes of the CGD donor are characterized by the absence of staining of cytochrome b_{558} subunits in a Western blot, a deletion of two nucleotides in exon 7 of the gene encoding for gp91-phox (deletion of two adenine-residues at positions 752/753) and an insertion of thymine at this position.

Human myeloperoxidase was isolated and purified from leukocytes (Bakkenist et al. 1987). A MPO solution in a 100 mM potassium phosphate buffer was measured in 0.6×0.6 mm square capillaries, with a 0.12 mm wall thickness.

The neutrophilic granulocytes were activated by addition of 0.1 μg/ml Phorbol-12-Myristate-13-Acetate (PMA, Sigma P-8139). Complete reduction of the redox centers inside the neutrophilic granulocytes was achieved by addition of sodium dithionite.

Escherichia Coli bacteria (ATCC 25922) were opsonized in serum for 30 minutes at 37 °C. The bacteria were added to the neutrophilic granulocytes after attachment to the quartz substrate.

A newly developed confocal direct imaging Raman microscope (CDIRM) (Sijtsema et al. 1998) was used to measure the Raman spectra (Fig. 2). The Raman microscope combines the possibility of confocal spectroscopy with confocal direct imaging. In the present study we have made use only of the spectroscopic mode. The following description will emphasize the performance of the confocal Raman microspectrometer. A krypton-ion laser (Coherent, Innova 90-K) and an argon-ion laser (Coherent, Innova 90-4) provide a choice of laserlines in the range between 413 to 799 nm. The laser-beam is reflected by a holographic beam-splitter (Kaiser Optical Systems Inc., Ann Arbor MI) and directed towards the microscope objective and the sample. The scattered light is collected by the same objective and transmitted through the beam-splitter. A holographic notch filter (Kaiser Optical Systems Inc., Ann Arbor MI) is used to suppress reflected laserlight and Rayleigh scattered light. The scattered light is focused onto an exchangeable pinhole at the entrance of a Jobin-Yvon HR460 imaging spectrograph (ISA, Jobin-Yvon, Paris, France). A 50 μm pinhole was used. The measurements were performed with a blazed holographic grating with 1200 l/mm (630 nm blaze) in the poly-chromator. The spectral resolution using an excitation wavelength of 413.1 nm was 2.5 cm^{-1}/pixel. A CCD detector, Princeton liquid nitrogen cooled back illuminated chip with 1100×330 pixels of 24×24 μm^2 (LN/CCD 1100 PB/VISAR, Princeton Instruments Inc., Trenton, N. J.) in combination with a 16-bit ST-130 controller, is placed in the focal plane of the exit port of the spectrograph.

The confocal properties of the Raman micro(spectro)meter have been extensively characterized (Sijtsema et al. 1998) for small spheres as well as for thin samples. For single cells the case of a small sphere is most relevant. Moving a sphere with a diameter of 0.282 μm through the focus gives rise to an axial resolution of 0.37 μm when a pinhole with a diameter of 50 μm is used. This resolution arises from a convolution of the diffraction limited spot (0.22 μm at 647.1 nm and NA = 1.2) and the sphere. The resolution of the setup is sufficient to distinguish positions inside the cytoplasm from positions at the cellular membrane. The location of enzymatic reactions can in this way be investigated. Absorption measurements were performed on a Shimadzu UV-2101PC spectrophotometer supplied with an integrating sphere to decrease the influence of light scattering on the extinction.

After isolation of the granulocytes a mixture of cells remains containing neutrophilic – and eosinophilic granulocytes. No stains are used to recognize the two cell types. Using the bright field microscope that is integrated with

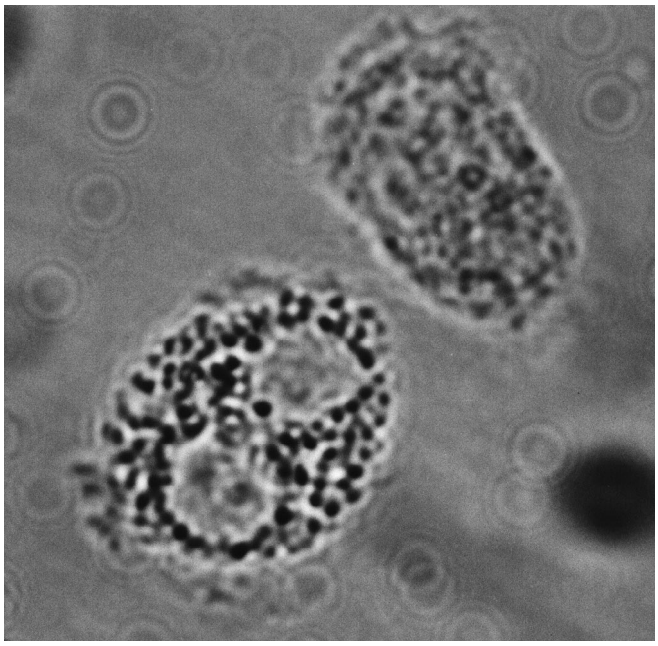

Fig. 3 A bright field image of a neutrophilic granulocyte and an eosinophilic granulocyte. In the eosinophilic granulocyte a nucleus with two lobes can easily be observed. Large granules fill the cytoplasma (*lower cell*). The nucleus of the neutrophilic granulocyte (*upper cell*) has a more complex shape and the granules in the cytoplasm are smaller. Using minimal amounts of laser light (~nanoW) during the selection of the position of measurement in the cell, areas with high granule concentration can easily be discerned from the elastic light scattering

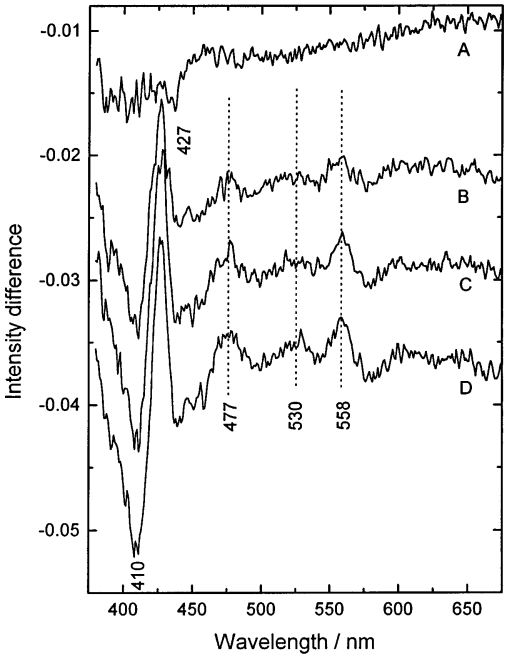

Fig. 4 Absorption difference spectra of neutrophilic granulocytes at varying time intervals after addition of PMA. The difference spectra are presented as {activated} – {non-activated}. *A* after 3 minutes, *B* after 5 minutes, *C* after 9 minutes and *D* after 11 minutes. Negative bands are due to oxidized Cb_{558} (410 nm), positive bands are due to reduced Cb_{558} (427, 530 and 558 nm) and reduced myeloperoxidase (477 nm) (See results and discussion). Spectra are shifted along the ordinate axis to avoid overlap

the Raman microscope the cells can be distinguished. The eosinophils in the mature phase appear to have two pronounced lobes. The nucleus particularly stands out against a large number of large granules in the cytoplasm. The desired neutrophilic granulocytes can be recognized by the nucleus that appears more polymorphonuclear (Fig. 3). The nucleus is less apparent than in the case of the eosinophils and the granules in the cytoplasm are smaller. The Raman spectra of the two cell types are strikingly different [Puppels et al. 1991 a] forming a final check on the identity of the cell. The spectra of neutrophilic granulocytes were measured by focusing the laser-beam in an area with a large concentration of granules inside the cell. These areas can easily be found using the intense scattering from the attenuated laser beam. Completely flat cells, which had adhered to the quartz plate, were not measured. The spectra of several cells were averaged to improve the signal to noise ratio and quartz and buffer signal were subtracted.

Difference spectra were calculated by subtracting spectra of the non-activated neutrophils from spectra of the PMA activated or dithionite reduced cells. Before calculating the difference spectra, the spectra of non-activated neutrophilic granulocytes were averaged over approximately 15 measurements, filtered with a fast Fourier transform filter and scaled on the 677 cm^{-1} band of the activated cell spectra. This scaling corrects for the differences in MPO or cytochrome b_{558} concentrations in the measurement volume in different cells.

Results

The stimulation of neutrophilic granulocytes with PMA results in distinct changes in the absorption spectra of the cells. The changes progress over time, starting approximately 10 minutes after the addition of PMA. The absorption spectra in Fig. 4 are presented as the spectra of {activated} minus {non-activated}. The decrease of oxidized Cb_{558} (negative band at 416 nm) and the increase of reduced Cb_{558} (positive band at 427 nm) as well as the increase of reduced (positive band at 477 nm) MPO is observed. Corresponding changes are observed in the Q-band region of the absorption spectrum around 550 nm.

In Fig. 5 the Raman spectrum of a neutrophilic granulocyte is presented (Fig. 5 C). The spectrum has been obtained using an excitation wavelength of 413.1 nm. The spectrum of neutrophilic granulocytes is well described by a sum of the Raman spectra of isolated specific (Fig. 5 A) and azurophilic granules (Fig. 5 B), showing that the spectrum from neutrophilic granulocytes results mainly from the resonant light scattering of CB_{558} and MPO (difference spectrum in Fig. 5 D). The position of the oxidation state marker bands at 1375 cm^{-1} for the specific granules and at 1370 cm^{-1} for the azurophilic granules confirms that the enzymes are in the oxidized state. The oxidation state marker band region of MPO around 1370 cm^{-1} results from the overlap of three bands that are similar in intensity. This

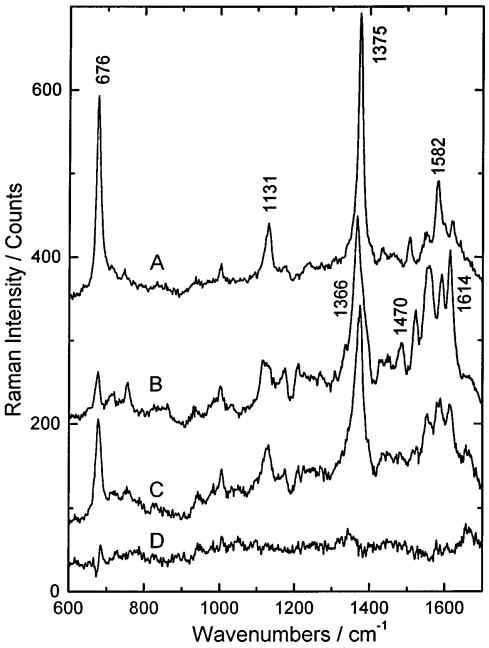

Fig. 5 Raman microspectroscopy of the specific and azurophilic granules from neutrophilic granulocytes. The excitation wavelength is at 413.1 nm. *A* The Raman spectrum of specific granules; *B* the Raman spectrum of azurophilic granules; *C* the Raman spectrum of a neutrophilic granulocyte; *D* the difference spectrum of {neutrophilic granulocyte} minus $\{c_1$*{azurophilic granule}+c_2*{specific granule}}. Most of the narrow bandwidth features in the spectrum of the neutrophilic granulocyte arise from cytochrome b_{558} (specific granule) and myeloperoxidase (azurophilic granule)

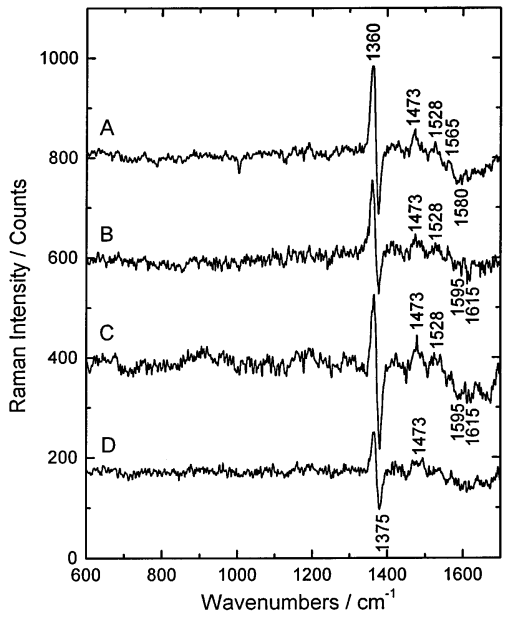

Fig. 7 Raman intensity difference spectra of neutrophilic granulocytes from a healthy individual. The difference spectra are presented as {reduced} – {native} in *A* or as {activated} – {non-activated} in *B*, *C* and *D*. Reduction in *A* is performed with dithionite solution. Activation in *B* is obtained by addition of PMA. Activation in *C* is obtained by addition of a high concentration of *Escherichia Coli* (ATCC 25922) and in *D* by a low concentration of *E. Coli*. The spectra are obtained in the cytoplasm of the neutrophilic granulocytes

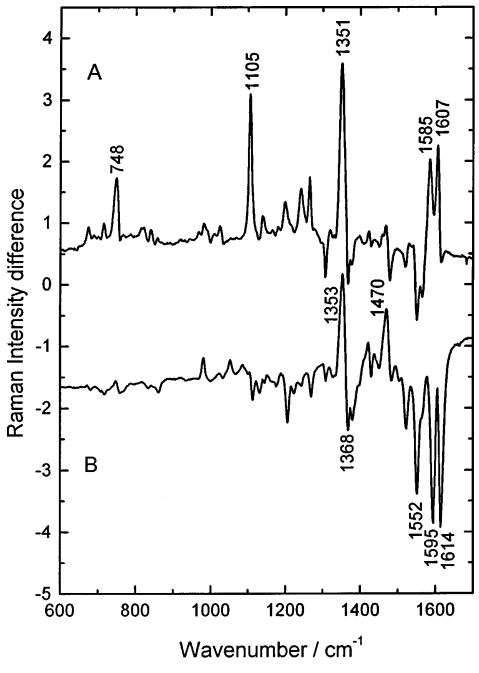

Fig. 6 Raman difference spectra of myeloperoxidase at two different excitation wavelengths. The difference spectra are presented as {reduced} – {oxidized}. The reduction of MPO is done by addition of dithionite to the solution of the oxidized MPO. *A* λ_{exc} = 457.9 nm; *B* λ_{exc} = 413.1 nm. Spectra are shifted along the ordinate axis to avoid overlap

pattern is the result of the low local symmetry of the porphyrin group in MPO. The porphyrin group is connected to the protein in three positions and it has been concluded (Kooter et al. 1997) that the covalent bond with methionine 243 is responsible for the spectroscopic properties and to some extent for the enzymatic properties of MPO.

The absorption spectra of Cb_{558} in the oxidized and reduced state and of MPO in the oxidized and reduced state suggest that a proper selection of the Raman excitation wavelength may help to distinguish the changes in the different compounds in single cells. Figure 6 shows Raman difference spectra of {Reduced MPO}-{oxidized MPO} at both 457.9 nm (Fig. 6 A) and 413.1 nm (Fig. 6 B). It can be observed that at both wavelengths large changes in the spectra of MPO occur as a result of a change in the oxidation state. The change in oxidation state is here achieved by addition of dithionite. Most notable are the changes in bands at 748, 1105, 1351, 1585 and 1607 cm^{-1} at an excitation wavelength of 457.9 nm and at 1353, 1470, 1595 and 1614 cm^{-1} at an excitation wavelength of 413.1 nm. This needs to be compared with the Raman spectra of Cb_{558} in the reduced and the oxidized state. The spectra of Cb_{558} at an excitation wavelength of 413.1 nm have been obtained (Hurst et al. 1991). The spectrum of the oxidized state is dominated by intense bands at 1375 and 676 cm^{-1}. Upon reduction the oxidation state marker band at 1375 cm^{-1} shifts to 1360 cm^{-1}. No spectra of Cb_{558} have been reported

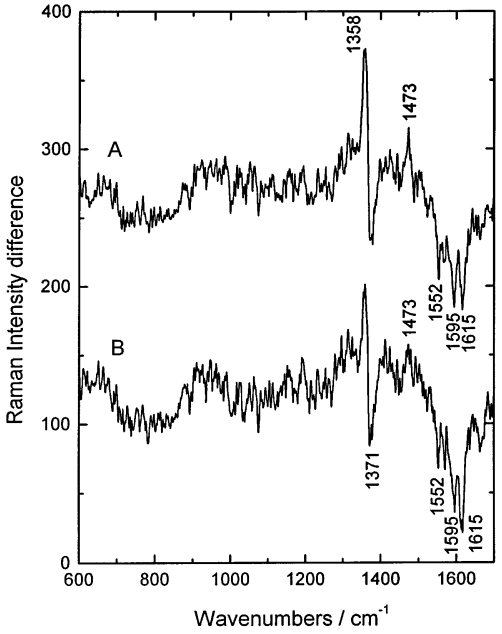

Fig. 8 Raman intensity difference spectra of neutrophilic granulocytes from a chronic granulomatous disease (CGD)-patient. *A* Neutrophilic granulocytes reduced with dithionite minus untreated cells; *B* neutrophilic granulocytes activated with E. Coli bacteria minus untreated cells

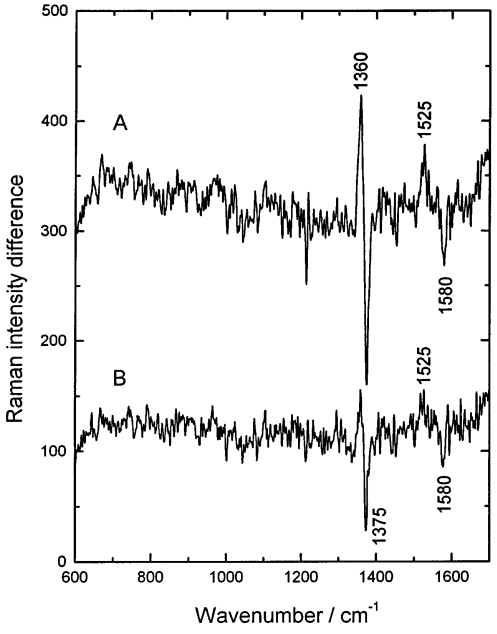

Fig. 9 Raman intensity difference spectra of neutrophilic granulocytes from a patient with a MPO deficiency. *A* Neutrophilic granulocytes reduced with dithionite minus untreated cells; *B* neutrophilic granulocytes activated with E. Coli bacteria minus untreated cells

with an excitation wavelength at 457.9 nm. We can conclude that oxidized Cb_{558} and MPO and reduced Cb_{558} and MPO can be distinguished on the basis of their Raman spectra excited with a laser wavelength of 413.1 nm.

Raman difference spectra of {activated} minus {non-activated} neutrophilic granulocytes of healthy individuals are presented in Fig. 7. The spectra are compared with the difference spectra from dithionite reduced cells (Fig. 7 A). In Fig. 7 B the activation is obtained with PMA. In Figs. 7 C and 7 D activation is obtained by addition of E. Coli bacteria to the neutrophilic granulocytes. The most pronounced changes in these spectra: the negative band at 1375 cm^{-1} (absence of oxidized MPO and oxidized Cb_{558}), a positive band at 1360 cm^{-1} (presence of reduced Cb_{588}), a positive band at 1473 cm^{-1} (reduced MPO), a positive band at 1525 cm^{-1} (reduced Cb_{558}) and a broad negative band at 1590 to 1620 cm^{-1} result from the decrease in oxidized MPO.

In Fig. 8 the neutrophilic granulocytes from a CGD patient are activated with E. Coli bacteria (Fig. 8 B). The Raman difference spectrum is compared with that obtained after dithionite reduction (Fig. 8 A). In the neutrophilic granulocytes no cytochrome b_{558} is present. All the observed redox state changes in the difference spectrum result from changes in MPO. They compare well with the expected difference spectrum from pure MPO (Fig. 6 B).

In Fig. 9 the neutrophilic granulocytes from a patient with MPO deficiency are activated with E. Coli bacteria (Fig. 9 B). The Raman difference spectrum is compared with that obtained after dithionite reduction (Fig. 9 A). In the neutrophilic granulocytes no myeloperoxidase is present. The most important changes in the Raman spectrum are the negative band at 1375 and 1580 cm^{-1} (oxidized cytochrome b_{558}) and the positive bands at 1360 and 1525 cm^{-1} (reduced cytochrome b_{558}), and they indicate redox state changes in cytochrome b_{558}.

Discussion

We have studied the response of neutrophilic granulocytes to activation with PMA or E. Coli bacteria using Raman microspectroscopy. This method provides detailled molecular information. The molecular cross section for this type of spectroscopy is small, resulting in a low signal rate. The power in the laser focus is approximately 2×10^9 W/m^2 (0.5 mW/0.25 μm^2). Cell viability is maintained (Puppels et al. 1991 b) as long as non-resonant excitation wavelengths (660 nm) are used. In the present study it was desirable to be selective for the enzymes Cb_{558} and MPO. This was achieved by resonance Raman excitation. In this case a bleaching could be observed, decreasing the time in which reliable signal accumulation can be performed. We found that a measurement time of 10 seconds per cell optimized between quality of the spectra and bleaching. Improvement of the signal-to-noise ratio was achieved by accumulation of 10 to 15 single cell measurements.

Activation of neutrophilic granulocytes with phorbol-12-myristate-13-acetate leads to a chain of molecular events. PMA activates protein kinase C (Majumdar et al. 1991). This leads to the phosphorylation of NADPH-oxidase (Dusi and Rossi 1993) and in turn stimulates the electron transfer in this system for the formation of superox-

ide anions. PMA does not lead to phagosome formation. Also, PMA does not directly influence the azurophilic granules and MPO inside the granules. Further, E. Coli bacteria are used. This activator must be considered to be able to start the formation of a phagosome by the neutrophilic granulocyte.

The activation with PMA or bacteria of single cells of neutrophilic granulocytes gives rise to clear changes in the micro-Raman spectra excited at 413.1 nm. These changes can be described as changes in the redox state of both cytochrome b_{558}, which is a part of the NADPH-oxidase complex and myeloperoxidase. The resonance conditions are slightly in favor of the cytochrome b_{558} resulting in stronger signal contributions from this complex. The relationship between the observed reactions is that Cb_{558} generates superoxide anion, O_2^-. This is converted by superoxide dismutase to hydrogen peroxide, H_2O_2. When MPO follows a peroxidase reaction H_2O_2 will act as a substrate. MPO compound I is a potent oxidizer of Cl^- and the formation of hypohalous acid, HOCl, will result as the major product of MPO. However O_2^- will also react directly with MPO to form compound III (Fig. 1) (Winterbourne et al. 1985). Subsequently molecular oxygen dissociates from compound III and reduced MPO will be formed. This is also observed in the absorption spectra (Fig. 4) and is in correspondence with the results from (Winterbourne 1985; Fig. 2 d). Also observed in the absorption spectrum is the occurrence of the reduction of Cb_{558}. This is expected when the oxygen supply to the cells is insufficient. The consequence for Cb_{558} is that the NADPH-oxidase complex shuttles electrons across the membrane with Cb_{558} at the receiving end. In the absence of oxygen Cb_{558} will be trapped in the reduced state.

The Raman difference spectra obtained with Raman microspectroscopy from single neutrophilic granulocyte cells present direct evidence of the formation of reduced MPO (Figs. 7 and 8) and of reduced Cb_{558} (Fig. 7 and 9). The expected difference spectrum for Cb_{558} can be deduced from Hurst et al. (1991). The spectrum contains minima at 1375 cm^{-1} and 1580 cm^{-1}, and maxima at 1360 and 1528 cm^{-1}. The expected difference spectrum, obtained at an excitation wavelength of 413.1 nm, for MPO is presented in Fig. 6 B. Maxima occur at 1353 and 1470 cm^{-1}. Minima occur at 1368, 1552, 1595 and 1614 cm^{-1}. As a result of the stronger resonance enhancement of the Raman spectrum of Cb_{558} than myeloperoxidase overlapping bands are dominated by Cb_{558} bands. This explains the occurrence in all spectra of a maximum at 1360 cm^{-1} and a minimum at 1375 cm^{-1}.

Activation of neutrophilic granulocytes from a healthy donor with PMA leads to a reaction of both Cb_{558} as well as myeloperoxidase, as is evidenced by the positive bands at 1360 and 1528 cm^{-1} (reduction of Cb_{558}), a positive band at 1473 cm^{-1} (reduction of myeloperoxidase) and negative bands at 1552, 1595 and 1614 cm^{-1} (reduction of myeloperoxidase). Corresponding changes are observed after activation with E. Coli bacteria. A high dose of bacteria (Fig. 7 C) results in quantitatively comparable changes as for dithionite reduction (Fig. 7 A). A low dose (factor 10 less) of bacteria gives rise to a weaker reaction from the neutrophilic granulocytes but the reduction of Cb_{558} and MPO is manifest. These experiments show that activation of single, living neutrophilic granulocytes can be followed using Raman microspectroscopy. In the short (10 sec) measurement time needed per cell all the acquired signal can be ascribed to the Raman scattering of cytochrome b_{558} and myeloperoxidase. Sufficient signal is obtained to visualize the changes after making difference spectra. Considering the measurement volume ($\sim 0.9\ \mu m^3$ with a depth resolution of 3.6 μm) of the confocal Raman microspectrometer (Sijtsema et al. 1998) it can be concluded that all the signal indeed originates from the cytoplasm of the neutrophilic granulocyte. This observation supports the notion that the activation causes an intra-cellular release of oxygen metabolites. The activation influences the Cb_{558} from the specific granules, which is as expected. It affects also MPO in the azurophilic granules suggesting a close relation between the different types of granules. This observation is in good agreement with the recent observation (Lundqvist et al. 1996) that PMA-induced chemi-luminescence was insensitive to extra-cellular scavengers of superoxide anion as well as hydrogen peroxide.

The activation with E. Coli bacteria of neutrophilic granulocytes from a patient with CGD gives rise to a difference spectrum (Fig. 2 B), which corresponds with the difference spectrum from MPO (Fig. 6 B). Although the neutrophilic granulocytes from such a patient do not contain the cytochrome b_{558} and hence, have no capacity through the NADPH-oxidase complex to produce oxygen metabolites an obvious reduction of MPO does take place. In principle, two explanations could explain the observed result. One explanation is that the bacteria produce superoxide anion and the second explanation is that the neutrophilic granulocyte has an alternative pathway to form superoxide anions. In work (Ahmed et al. 1991) on HL-60 cells it is reported that these cells do not contain specific granules but are capable, albeit at a low efficiency, of generating superoxide anions and hydrogen peroxide after stimulation with PMA. No such effect is known for healthy neutrophilic granulocytes. It is not known whelter neutrophilic granulocyte from patients with CGD (gp91-phox) have optimized a different pathway to produce superoxide anion. These cells will then still be capable of employing MPO as a bactericidal agent and activation will result in the difference spectra observed (Fig. 2 B).

Neutrophilic granulocytes with MPO-deficiency can also be activated with E. Coli bacteria (Fig. 9 B). The cells contain specific granules with the NADPH-oxidase complex. The cytochrome b_{558} is reduced giving rise to the typical spectral pattern for the conversion of oxidized to reduced Cb_{558}.

Conclusion

The general conclusion from this paper is that enzymatic reactions related to the phagocytic process in neutrophilic

granulocytes can be investigated on a single cell basis with confocal Raman microspectroscopy. With this technique it is possible to distinguish cytochrome b_{558} and myeloperoxidase, two important enzymes in the pathway of the production of bactericidal agents. In the resting cell these compounds are in the oxidized state. Activation of the neutrophilic granulocyte with PMA or E. Coli bacteria leads to changes in the redox state of these enzymes, which can be directly recognized with Raman microspectroscopy. Using measurement times of 10 seconds and an excitation wavelength of 413.1 nm typical Raman spectra of the cell are obtained that can be ascribed to the light scattering of cytochrome b_{558} and myeloperoxidase. We have further substantiated this by comparing the spectrum of a neutrophilic granulocyte with that from specific – and azurophilic granules. We conclude from the present work that the changes in the redox state of both cytochrome b_{558} and myeloperoxidase occur intra-cellularly. Neutrophilic granulocytes from a CGD patient {gp91-phox} seem to be capable of generating superoxide. Important questions that stand out are the type of reactions that occur, the sequence of the reactions, the location of the reactions, the relationship between the different granules after activation, the delay in the occurrence of reactions and the quantitative extent of the reactions involving Cb_{558} and myeloperoxidase. Application of microscopic and microspectroscopic techniques will contribute to our understanding of these questions.

Acknowledgements We thank Mrs. I. Segers-Nolten for her assistance in the preparation of the cell samples, dr. Ingeborg Kooter and dr. Ron Wever of the Dept. of Biochemistry in the E. C. Slater Institute of the University of Amsterdam for helpful discussions and Dr. Arthur Verhoeven of the Central Blood Laboratory of the Netherlands, Red Cross Blood Transfusion service in Amsterdam for the donation of cellular material of CGD- and MPO-deficient patient material. We declare that to the knowledge of the authors the experiments described in this manuscript are performed in accordance with the current laws in the Netherlands.

References

Ahmed N, Williams JF, Weidemann MJ (1991) The human promyelocytic HL-60 cell line: a model of myeloid cell differentiation using dimethylsulphoxide, phorbol ester and butyrate. Biochem Int 23: 591 – 602

Babior BM (1978) Oxygen-dependent microbial killing by phagocytes. New Engl J Med 298: 659 – 668

Bakkenist ARJ, Wever R, Vulsma T, Plat H, Gelder van BF (1987) Isolation procedure and some properties of myeloperoxidase from human leucocytes. Biochim Biophys Acta 524: 45 – 54

Bjerrum OW, Borregaard N (1989) Dual granule localization of the dormant NADPH oxidase and cytochrome b_{558} in human neutrophils. Eur J Haematol 43: 67 – 77

Bolscher BGMJ, Denis SW, Verhoeven AJ, Roos D (1990) The activity of one soluble component of the cell-free NADPH: O_2 oxidoreductase of human neutrophils depends on guanosine 5′-O-(3-thio)triphosphate. J Biol Chem 265: 15 782 – 15 787

Brederoo P, Meulen van der J, Mommaas-Kienhuis AM (1983) Development of the granule population in neutrophil granulocytes from human bone marrow. Cell Tissue Res 234: 469 – 496

Cross AR, Curnutte JT (1995) The cytosolic activating factor $p47^{phox}$ and $p67^{phox}$ have distinct roles in the regulation of electron flow in NADPH oxidase. J Biol Chem 270: 6543 – 6548

Cross AR, Heyworth PG, Rae J, Curnutte JT (1995) A variant X-linked chronic granulomatous disease patient ($\times 91^{+}$) with partially functional cytochrome b. J Biol Chem 270: 8194 – 8200

Dusi S, Rossi F (1993) Activation of NADPH oxidase of human neutrophils involves the phosphorylation and the translocation of cytosolic $p67^{phox}$. Biochem J 296: 367 – 371

Hurst JK, Loehr TM, Curnutte JT, Rosen H (1991) Resonance Raman and electron paramagnetic resonance structural investigations of neutrophil cytochrome b_{558}. J Biol Chem 266: 1627 – 1634

Jesaitis AJ, Buescher ES, Harrison D, Quinn MT, Parkos CA, Livesey S, Linner J (1990) Ultrastructural localization of cytochrome b in the membranes of resting and phagocytosing human granulocytes. J Clin Invest 85: 821 – 835

Kooter IM, Moguilevsky N, Bollen A, Sijtsema NM, Otto C, Wever R (1997) Site-directed mutagenesis of Met243, a residue of myeloperoxidase involved in binding of the prosthetic group. J Biol Inorg Chem 2: 191 – 197

Long DA (1977) Raman spectroscopy, 1st edn. McGraw-Hill, New York USA

Lundqvist H, Follin P, Khalfan L, Dahlgren C (1996) Phorbol myristate acetate-induced NADPH oxidase activity in human neutrophils: only half the story has been told. J Leukocyte Biol 59: 270 – 279

Majumdar S, Rossi MW, Fujiki T, Phillips WA, Disa S, Queen CF, Johnston RB, Rosen OM, Corkey BE, Korchak HM (1991) Protein kinase C isotypes and signaling in neutrophils. J Biol Chem 266: 9285 – 9294

Marquez LA, Huang JT, Dunford HB (1994) Spectral and kinetic studies on the formation of myeloperoxidase compounds I and II: roles of hydrogen peroxide and superoxide. Biochemistry 33: 1447 – 1454

Nauseef WM (1990) Myeloperoxidase deficiency. Hematol Pathol 4: 165 – 178

Puppels GJ, Garritsen HSP, Segers-Nolten GMJ, Mul de FFM, Greve J (1991 a) Raman microspectroscopic approach to the study of human granulocytes. Biophys J 60: 1046 – 1056

Puppels GJ, Olminkhof JHF, Segers-Nolten GMJ, Otto C, Mul de FFM, Greve J (1991 b) Laser irradiation and Raman spectroscopy of single living cells and chromosomes: sample degradation occurs with 514.5 nm but not with 660 nm laser light. Exp Cell Res 195: 361 – 367

Sijtsema NM, Wouters SD, Grauw de CJ, Otto C, Greve J (1998) A confocal direct imaging Raman microscope: design and applications in biology. Applied Spectr 52 (in press)

Winterbourne CC, Garcia RC, Segal AW (1985) Production of the superoxide adduct of myeloperoxidase (compound III) by stimulated human neutrophils and its reactivity with hydrogen peroxide and chloride. Biochem J 228: 583 – 592

Yazdanbakhsh M, Eckmann CM, Koenderman L, Verhoeven AJ, Roos D (1987) Eosiniphils do respond to fMLP. Blood 70: 379 – 383